Self-referenced technique for monitoring and analysing the non-linear dynamics of semiconductor lasers

Christophe Gosset,[1,*] Ivan Aldaya,[2] Cheng Wang,[1,3] Heming Huang,[1] Xin You,[1] Jacky Even,[3] Gabriel Campuzano,[2] and Frédéric Grillot[1]

[1]*TELECOM ParisTech, Ecole Nationale Supérieure des Télécommunications, and CNRS, LTCI, 46, rue Barrault, 75634 Paris Cedex France*

[2]*Department of Electrical and Computational Engineering, Tecnologico de Monterrey, Monterrey, NL, 64849 Mexico*

[3]*Université Européenne de Bretagne, Laboratoire CNRS FOTON, INSA, 20, avenue des buttes de Coesmes, 35043 Rennes Cedex, France*

[*]*christophe.gosset@telecom-paristech.fr*

Abstract: We propose in this paper a self-referenced method based on asynchronous sampling to monitor the waveform of periodic and quasi-periodic signals, with a low number of samples, typically 2^{14} or lower. It provides a high-resolution representation of the signal under test, representative of the analog intensity signal under test. Additionally, the proposed approach is robust to the timing jitter of the signal, as experimentally demonstrated. Such features enable the accurate display of periodic and quasi-periodic signals. The method is applied to the characterization of laser dynamics, such as time series and phase portrait of periodic nonlinear regimes in optically injected lasers.

OCIS codes: (120.0120) Instrumentation, measurement, and metrology; (140.3520) Lasers, injection-locked; (140.5960) Semiconductor lasers.

References and links

1. L. Noirie, F. Cerou, G. Mostakides, O. Audouin, and P. Peloso, "New transparent optical monitoring of the eye diagram and BER using asynchronous under-sampling of the signal," in Proc. European Conference on Optical Communication (ECOC), PD2.2 (2002)
2. M. Westlund, H. Sunnerud, M. Karlsson, and P. A. Andrekson, "Software-synchronized all-optical sampling for fiber communication systems," J. Lightwave Technol. **23**(3), 1088–1099 (2005).
3. M. Sköld, M. Westlund, H. Sunnerud, and P. A. Andrekson, "All-optical waveform sampling in high-speed optical communication systems using advanced modulation formats," J. Lightwave Technol. **27**(16), 3662–3671 (2009).
4. C. Dorrer, C. R. Doerr, I. Kang, R. Ryf, J. Leuthold, and P. J. Winzer, "Measurement of eye diagrams and constellation diagrams of optical sources using linear optics and waveguide technology," J. Lightwave Technol. **23**(1), 178–186 (2005).
5. M. Virte, K. Panajotov, H. Thienpont, and M. Sciamanna, "Deterministic polarization chaos from a laser diode," Nat. Photonics **7**(1), 60–65 (2012).
6. S. Wieczorek, B. Krauskopf, T. Simpson, and D. Lenstra, "The dynamical complexity of optically injected semiconductor lasers," in *Physics Report* (Elsevier, 2005)
7. D. M. Kane and K. A. Shore, *Unlocking Dynamic Diversity* (Wiley, 2005).
8. J.-M. Liu, H.-F. Chen, and S. Tang, "Dynamics and Synchronization of Semiconductor Lasers for Chaotic Optical,"*Digital Communications Using Chaos and Nonlinear Dynamics Institute for Nonlinear Science* (Springer, 2006), Chap. 10, pp. 285–340.
9. J. P. Toomey, C. Nichkawde, D. M. Kane, K. Schires, I. D. Henning, A. Hurtado, and M. J. Adams, "Stability of the nonlinear dynamics of an optically injected VCSEL," Opt. Express **20**(9), 10256–10270 (2012).
10. M. Selmi, C. Gosset, M. Noelle, P. Ciblat, and Y. Jaouen, "Blockwise digital signal processing for Polmux QAM/PSK optical coherent systems," J. Lightwave Technol. **29**(20), 3070–3082 (2011).
11. P. Ciblat, P. Loubaton, E. Serpedin, and G. B. Giannakis, "Performance analysis of blind carrier frequency offset estimators for non-circular transmissions through frequency-selective channels," IEEE Trans. Signal Process. **50**(1), 130–140 (2002).
12. K. Lüdge, *Nonlinear Laser Dynamics - From Quantum Dots to Cryptography* (Wiley, 2012).

#205142 - $15.00 USD Received 21 Jan 2014; revised 4 Mar 2014; accepted 4 Mar 2014; published 27 Jun 2014

13. R. Lang, "Injection locking properties of a semiconductor laser," IEEE J. Quantum Electron. **18**(6), 976–983 (1982).
14. O. Lidoyne, P. Gallion, C. Chabran, and G. Debarge, "Locking range, phase noise and power spectrum of an injection- locked semiconductor laser," IEE Proceedings Journal of Optoelectronics, **137**, 147–154, (1990).
15. Y. Yamamoto and T. Kimura, "Coherent optical fiber transmission systems," IEEE J. Quantum Electron. **17**(6), 919–935 (1981).
16. S. Mohrdiek, H. Burkhard, and H. Walter, "Chirp reduction of directly modulated semiconductor lasers at 10 Gb/s by strong CW light injection," J. Lightwave Technol. **12**(3), 418–424 (1994).
17. X. J. Meng, T. Chau, and M. C. Wu, "Improved intrinsic dynamic distortions in directly modulated semiconductor lasers by optical injection locking," IEEE Trans. Microw. Theory Tech. **47**(7), 1172–1176 (1999).
18. T. B. Simpson and J. M. Liu, "Enhanced modulation bandwidth in injection-locked semi- conductor lasers," IEEE Photon. Technol. Lett. **9**(10), 1322–1324 (1997).
19. J. M. Liu, H. F. Chen, X. J. Meng, and T. B. Simpson, "Modulation bandwidth, noise, and stability of a semiconductor laser subject to strong injection locking," IEEE Photon. Technol. Lett. **9**(10), 1325–1327 (1997).
20. E. K. Lau, X. Zhao, H.-K. Sung, D. Parekh, C. Chang-Hasnain, and M. C. Wu, "Strong optical injection-locked semiconductor lasers demonstrating > 100-GHz resonance frequencies and 80-GHz intrinsic bandwidths," Opt. Express **16**(9), 6609–6618 (2008).
21. N. A. Olsson, N. A. Olsson, H. Temkin, R. A. Logan, L. F. Johnson, G. J. Dolan, J. P. van der Ziel, and J. C. Campbell, "Chirp-free transmission over 82.5 km of single mode 29 fibers at 2 Gbit/s with injection locked DFB semiconductor lasers," J. Lightwave Technol. **3**(1), 63–67 (1985).
22. A. Kaszubowska, P. Anandarajah, and L. P. Barry, "Improved performance of a hybrid radio/fiber system using directly modulated laser transmitter with external injection," IEEE Photon. Technol. Lett. **14**(2), 233–235 (2002).
23. T. B. Simpson and F. Doft, "Double-locked laser diode for microwave photonics applications," IEEE Photon. Technol. Lett. **11**(11), 1476–1478 (1999).
24. X. Q. Qi and J. M. Liu, "Photonic microwave applications of the dynamics of semiconductor lasers," IEEE J. Sel. Top. Quantum Electron. **17**(5), 1198–1211 (2011).
25. M. Al-Mumin, X. Wang, W. Mao, S. A. Pappert, and G. Li, "Optical generation and sideband injection locking of tunable 11-120GHz microwave/millimeter signals," Electron. Lett. **36**(18), 1547–1548 (2000).
26. S. C. Chan and J. M. Liu, "Microwave frequency division and multiplication using an optically injected semiconductor laser," IEEE J. Quantum Electron. **41**(9), 1142–1147 (2005).
27. Y. S. Yuan and F. Y. Lin, "Photonic generation of broadly tunable microwave signals utilizing a dual-beam optically injected semiconductor laser," IEEE Photon. J. **3**(4), 644–650 (2011).
28. T. B. Simpson and F. Doft, "Double-locked laser diode for microwave photonics applications," IEEE Photon. Technol. Lett. **11**(11), 1476–1478 (1999).
29. C. H. Chu, S. L. Lin, S. C. Chan, and S. K. Hwang, "All-optical modulation format conversion using nonlinear dynamics of semiconductor lasers," IEEE J. Quantum Electron. **48**(11), 1389–1396 (2012).
30. C. Cui, X. Fu, and S. C. Chan, "Double-locked semiconductor laser for radio-over-fiber uplink transmission," Opt. Lett. **34**(24), 3821–3823 (2009).
31. Y. H. Hung, C. H. Chu, and S. K. Hwang, "Optical double-sideband modulation to single-sideband modulation conversion using period-one nonlinear dynamics of semiconductor lasers for radio-over-fiber links," Opt. Lett. **38**(9), 1482–1484 (2013).
32. H.-H. Lu, H.-H. Huang, H.-S. Su, and M.-C. Wang, "Fiber optical CATV system-performance improvement by using external light-injection technique," IEEE Photon. Technol. Lett. **15**(7), 1017–1019 (2003).
33. M. Pochet, N. A. Naderi, Y. Li, V. Kovanis, and L. F. Lester, "Tunable photonic oscillators using optically injected quantum-dash diode lasers,'," IEEE Photon. Technol. Lett. **22**(11), 763–765 (2010).
34. T. B. Simpson, J. M. Liu, M. AlMulla, N. G. Usechak, and V. Kovanis, "Linewidth sharpening via polarization-rotated feedback in optically-injected semiconductor laser oscillators," IEEE J. Sel. Top. Quantum Electron. **19**(4), 1500807 (2013).
35. J. P. Zhuang and S. C. Chan, "Tunable photonic microwave generation using optically injected semiconductor laser dynamics with optical feedback stabilization," Opt. Lett. **38**(3), 344–346 (2013).
36. M. T. Crowley, N. A. Naderi, H. Su, F. Grillot, and L. F. Lester, "GaAs based Quantum Dot Lasers," Adv. Semicond. Lasers **86**, 371–417 (2012).
37. I. A. Murakami, "Phase Locking and Chaos Synchronization in injection-Locked Semiconductor Lasers," IEEE J. Quantum Electron. **39**(3), 438–447 (2003).

1. Introduction

In the field of optics and optical communications, hybrid optical-electrical asynchronous sampling technique is a powerful tool for the monitoring of periodic and digital data stream even at very high symbol rates [1–4]. In the domain of semiconductor devices, nonlinear dynamical scenario occurring in a laser diode operating with or without external control has been the field of extensive theoretical studies over the last twenty years, leading to the

#205142 - $15.00 USD Received 21 Jan 2014; revised 4 Mar 2014; accepted 4 Mar 2014; published 27 Jun 2014

generation and the applications of periodic optical signals [5,6]. In an optically-injected laser, it is known that the laser can exhibit various dynamical regimes such as periodic, quasi-periodic and even chaotic regimes. As a consequence of that, monitoring and analyzing the nonlinear dynamical features is of first importance since it can enable insights for various engineering applications. The experimental extraction of the nonlinear dynamical features is not intensively studied as for instance described in references [7–9]. Most of the work is done theoretically but a very little is done experimentally. Most traditionally, the monitoring of the nonlinear dynamics is realized through a sampling oscilloscope coupled to a clock recovery. However, because the latter can modify the temporal statistic, it is not always possible to get a precise analysis of the laser output. As opposed to that, in this paper we propose a temporal real-time asynchronous sampling scheme associated with proper digital signal processing for a detailed characterization of a dynamical system, such as a laser diode operating under optical injection. It concatenates a lot of advantages such as a no time reference, real-time acquisition, no interpolation operation, and high robustness against the timing jitter.

With this technique the first aim to display the waveform of a periodic signal, or the eye diagram of a digital data modulated signal, is the recovery of the signal period with regards the sampling period [2]. We denote this operation as *clock recovery*, which is explained in the next section. In this paper, we propose an all-digital block-wise clock recovery based on the spectral analysis of the asynchronously sampled signal. Due to its block structure, the proposed algorithm appears to be robust to the timing fluctuations of the signal. Finally, it provides a rapid convergence with only 2^{14} samples.

The paper is organized as follow: we will first present the asynchronous sampling context and the principle of the clock recovery. Next, we will evaluate the experimental performances of the clock recovery with a known period varying signal, comprised of a polarization scrambler concatenated with a Polarization Maintaining Fiber (PMF). The method is then applied to the blind recovery of the periodic temporal signal emitted by an injected semiconductor laser. Period one (P1) and period doubling (P2) dynamical regimes are investigated. Several sampling frequencies are used in order to show the important jitter of the signal generated under these optical injection regimes. This paper is of first importance because it reports a novel experimental method devoted to the extraction of the various periodical regimes. The proposed technique, which relies on a digital signal processing of an asynchronous sampled signal without any interpolation operation gives clear evidence of typical nonlinear dynamical features, which can be exploited for optical telecommunications networks.

2. Asynchronous sampling context and principle of the digital clock recovery

We present in this section the principle of operation of asynchronous sampling and the parameters required to recover the intensity waveform of a periodic signal sampled asynchronously. The tools used in this section come from digital signal processing and offset frequency estimation theories [10,11]. We focus our efforts in this section to provide the main results that are of great interest to extract relevant parameters in order to monitor physical dynamical systems without any clock reference signal between the measurement system and the signal under test (SUT).

The optical signal to analyse, coming from an optical dynamical system, is detected with a square law photodiode. The detected signal $I_D(t)$ is proportional to the intensity of the optical field to analyse, of period T_D. $I_D(t)$ is an analogic signal, sampled at a period T_S with an Analog-to-Digital Converter (ADC). At the output of the ADC, the signal is discrete, and it corresponds to the samples provided at instant t-nT_S of the intensity given by:

$$r_S(n) = I_D(t - nT_S). \tag{1}$$

The sampling period is related to the SUT period by the simple relation $T_S = kT_D + dt$, where k is either null (over sampling configuration) or a positive integer (under sampling

#205142 - $15.00 USD Received 21 Jan 2014; revised 4 Mar 2014; accepted 4 Mar 2014; published 27 Jun 2014

configuration). In an asynchronous sampling configuration, dt is a real non null value and the sampling frequency remains constant during the entire acquisition time.

The received discrete signal r_S strongly depends on the T_S/T_D ratio and, more precisely, on the normalized temporal step $\delta t/T_D$. From a spectral viewpoint, the impact of the T_S/T_D ratio is clearly exhibited by the frequency position of the fundamental frequency of r_s. If $dt = 0$, the sampled signal $r_S(n)$ is constant, and its spectrum consists of one component located at the zero frequency. If $dt = \varepsilon << T_D$, the raw data could provide an accurate representation of the analog waveform I_D, as a stroboscope. In this case, the fundamental frequency is nearly close to zero. The increase of dt/T_D induces an increase of the frequency position of the fundamental spectral component of r_S. To sum-up, $\delta t/T_D$ is related to the fundamental frequency position f_p for periodic signal by the following relationship:

$$\frac{dt}{T_D} = \frac{f_p}{N}, \tag{2}$$

Its value is in the $[0:1/2]$ range. Actually, dt/T_D sets the resolution of the raw data, which is apriori unknown. Nevertheless, whatever the value of dt/T_D, it is possible to obtain a high-resolution representation of the analog waveform I_D from the set of raw data, by superimposing all the samples in the same time slot $[0,T_D]$. To do that, the normalized temporal step dt/T_D is the key parameter to determine. Actually, it allows to re-localize the sample within the same period. To plot the signal along P periods, the normalized abscissae of each sample $r_s(n)$ as to be tuned to

$$t(n) = \left(n \frac{dt}{T_D} \right) \bmod P, \tag{3}$$

where *mod* is the modulo operator. It is thus important to estimate the normalized temporal step size with accuracy. Digital methods based on the calculation of periodogram had already been proposed to estimate $\delta t/T_D$ in the context of asynchronous sampling [1,2]. Nevertheless, the proposed methods do not address the monitoring of signals generated by an optical source affected by a strong jitter with a low number of samples. We propose in this section, a purely spectral method to estimate accurately dt/T_d using a block of raw data. It aims for the estimation of the relative frequency f_p, which according to (2) allows the recovery of dt/T_d.

The simple use of the Discrete Fourier Transform (DFT) to compute the spectrum $S(f)$ of a block of N data $r_S(n)$ provides an estimation of f_p with an accuracy proportional to $1/N$, corresponding to the frequency resolution of $S(f)$ [11], with $S(f)$ defined as the square modulus of the DFT

$$S(f) = \frac{1}{N} \left| \sum_{n=0}^{N-1} r_S(n) \exp(2i\pi nf) \right|^2. \tag{4}$$

$S(f)$ is an N element frequency signal, with f a normalized frequency in the range [-1/2; + 1/2]. In the under-sampling configuration, $S(f)$ is affected by aliasing as the frequency sampling is lower than the bandwidth of the SUT. As a consequence, the fundamental frequency of the SUT is in general not the lower spectral component of $S(f)$. It is important to note that f_p must correspond to the fundamental frequency of the SUT in order to plot the reconstructed signal without any artefact.

Most of the time, and for a block size not to large ($N<2^{15}$ for instance), the error estimation is not low enough to plot the reconstructed signal using (3) without adding significant deterministic jitter induced by the estimation technique. We propose to reduce the estimation error by computing an optimization technique using the Newton algorithm for fast convergence

#205142 - $15.00 USD Received 21 Jan 2014; revised 4 Mar 2014; accepted 4 Mar 2014; published 27 Jun 2014

$$f_p(k+1) = f_p(k) + \mu \left[\frac{\partial S}{\partial f} \Big)_{f_p(k)} \Big/ \frac{\partial^2 S}{\partial f^2} \Big)_{f_p(k)} \right] \quad (5)$$

S(f) corresponds to the cost function of the algorithm, and μ the step size which depends on the block size. As the SUT is real, *S(f)* is symmetric according to the zero frequency. Hence, the initialization of the algorithm is achieved by finding the normalized frequency maximizing (4) in the range]0:1/2] (or [-1/2:0[). This optimization technique reduces the estimation error to $1/N^3$, which is substantially lower than $1/N$, obtained when only the initialization value is used [11]. This improvement allows the accurate display of periodic signals, including time series and phase portrait of nonlinear dynamical systems. It is important to note that the first and second order derivatives involved in Eq. (5) can be computed exactly using the set of raw data.

We presented in this section the principle of operation for the waveform recovery scheme by using a periodic SUT, which corresponds to the kind of signal to analyse in the field of optical dynamical systems. The proposed method is also well adapted to monitor the waveform of optical digital communication data flow, even with infinite sequence length, in order to depict eye diagram. In this case, the periodicity to retrieve is related to the symbol period, or bit period for binary signal [1–4]. For such digital signals, the spectrum of the set of raw data given by (4) doesn't exhibit any pure spectral component related to the symbol rate, due to spectral aliasing. Nevertheless, it has been shown that the spectrum of $r_s^Q(n)$ exhibits a pure spectral component related to the symbol rate. Q is an integer depending on the digital modulation format of the incoming signal $r_s(n)$. For M-PSK signals, $Q = M$, for QAM, $Q = 4$, and for intensity modulated signal $Q = 2$ [10,11].

In the following, the proposed method will be applied to monitor a digital intensity modulated signal impaired by bit period variation and dynamical regimes of an optically injected diode laser.

3. Experimental demonstration of the performance of the monitoring scheme applied to a modulated signal impaired by random period variations

In the previous section we introduced the principle of operation to retrieve the waveform of an asynchronously sampled signal based on the block analysis of a set of raw data $r_s(n)$. We show in this section that the proposed method is robust to random period variation of the SUT. For this purpose, we built an experimental setup to generate such timing impairments. The SUT is an optical No Return to Zero (NRZ) digital data flow at 11.57 Gb/s generated with a Mach-Zehnder modulator driven by a 2^{15}-1 Pseudo Random Bit Sequence generator. It is then launched in an all-optical scheme to dynamically modify the bit period: we concatenated a polarization scrambler, with a maximum frequency scrambling of 200 kHz, and a 25m-length Polarization Maintaining Fibre (PMF). The SUT is then detected with a 10 GHz bandwidth AC-coupled photodiode and sampled with a 16 GHz bandwidth analogue-to-digital converter (ADC) operating at 62.5 MSamples/s. The estimation of dt/T_D parameter is done with 2^{14} samples. The block duration is about 260 µs, which is much longer than the minimum scrambling period of 5 µs. The SUT is thus strongly impaired by the scrambling scheme.

#205142 - $15.00 USD Received 21 Jan 2014; revised 4 Mar 2014; accepted 4 Mar 2014; published 27 Jun 2014

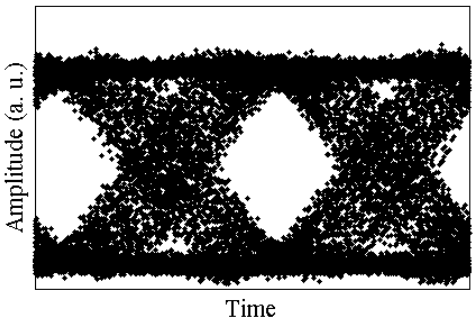

Fig. 1. Eye diagram after polarization scrambling and PMF (20k samples). Inset: eye diagram in back-to-back configuration (without scrambler), using the estimation of dt/T_D when scrambler was used.

We show in Fig. 1 the obtained eye diagram after estimation of the temporal step. As expected it exhibits a strong timing jitter, leading to the closure of the eye diagram. Nevertheless, we cannot affirm that it corresponds only to the fluctuations related to the scrambling scheme. In order to verify the robustness of the method against the timing jitter of the SUT, we show on the inset of Fig. 1 the eye diagram in the back-to-back (i.e. before the scrambling scheme) obtained with the estimation of $\delta t/T_D$ in the configuration of the timing jitter impairments. We observe an eye diagram with the same quality compared to the one obtained by estimating $\delta t/T_D$ in the back-to-back configuration. There is no impact on the eye diagram induced by the estimation technique in the presence of timing jitter. Hence, the clock recovery is very tolerant to timing fluctuations, and Fig. 1 shows only the timing fluctuations induced by the scrambling scheme.

For a sampling frequency of 62.5 MSamples/s, we observe the impact of the scrambling scheme during the transition between the two logical levels. It is important to note that the sampling frequency used in this experiment is not the lowest possible. In our case we choose a sampling frequency of 62.5 MSamples/s from a pedagogical viewpoint. For lower sampling frequency, the reconstructed eye diagram would have been completely blurred, illustrating the strong period variation of the SUT along the block duration, but such a figure would be considerably less informative to the reader. In the next sections, the sampling frequency is not set to the minimum allowed by the method. It is chosen to set the "amount" of timing jitter during the block duration. For instance, to only recover the waveform without taking into account the timing jitter of the SUT, the sampling frequency will be set to the highest possible value. On an other hand, if the goal of the measurement is to estimate or demonstrate the presence of timing jitter in the SUT, the sampling frequency will be reduced, but adapted to the value of the timing jitter.

4. Application to the extraction of the dynamical properties of optically-injected diode lasers

Optical injection in semiconductor lasers involves two optical sources, referred to as the master and slave lasers [9]. The master laser (ML) is typically a high-power single-mode sharp-linewidth tunable laser, which is injected into the slave laser (SL) cavity, thereby affecting its dynamical response and inherent free-running characteristic parameters in particular the relaxation oscillation frequency (typically above 1 GHz). In an optically-injected diode laser, it is well-established that the diode laser can exhibit various dynamical states [7,12]. Thus, when the locking conditions are satisfied, the frequency of the slave is locked to that of the master with a constant phase offset. There are two primary injection-locking parameters: optical frequency detuningΔf, and external injection ratio, R_{ext}. Frequency detuning is defined as the frequency offset between master and slave laser. The external

#205142 - $15.00 USD Received 21 Jan 2014; revised 4 Mar 2014; accepted 4 Mar 2014; published 27 Jun 2014

injection ratio is the master to slave power ratio at the slave's emitting facet. As the frequency of the master is changed, the slave mode will follow that frequency until the system becomes unlocked. The locking range is known to depend on several parameters, including the external power ratio, the coupling coefficient and the linewidth enhancement factor (α-factor) of the slave laser [13,14]. From a nonlinear dynamics viewpoint, the stable-locked state is created in a saddle-node bifurcation while further the relaxation oscillations become undamped via a Hopf-bifurcation, creating a limit cycle referred as period one (P1), which may further bifurcate via period-doubling (P2) route into chaos as the detuning and/or injection level are varied [7,12]. P1 limit cycle state is characterized by the presence of undamped relaxation oscillation sidebands, while P2 shows the occurrence of additional relaxation oscillation side-bands associated with pulsating at half the slave laser's characteristic relaxation oscillation frequency [7].

Over the last years, the injection-locking technique has been shown to offer various advantages especially in the field of coherent optical communications [15]. Based on the stable-locked region, the improvements to the modulated free-running directly modulated slave laser include an enhancement in the relaxation oscillation, a reduction in the laser relative intensity-to-noise (RIN), a reduction of the nonlinear distortion, and most importantly, a decrease in the linewidth and frequency chirping [16–19]. Using optical injection-locking, a narrowband response with larger than 80 GHz intrinsic bandwidth has been reported in a quantum well (QW) vertical cavity surface emitting laser (VCSEL) operating at 1510 nm [20]. One important figure of merit in directly modulated free-running lasers is the bit rate-length (BL) product. Limited transmission distances in optical fiber links are mainly due to the linewidth broadening caused by frequency chirping. Reduced frequency chirp by injection-locking decreases the linewidth broadening thereby reducing the pulse broadening caused by dispersive fibers. This important feature of injection-locking was reported to create low chirp, allowing for long-haul transmission with improved bit rate-length product [21,22]. On the other hand, P1 oscillations have been used for the generation of photonic microwaves that can be continuously tuned over a very large frequency range, as well as for AM-to-FM signal conversion and remote target detection [23,24]. As a consequence of that, the external control technique of free-running lasers through optical injection-locking has recently been implemented in several state-of-the-art applications including millimetre- and microwave-wave generation [25–28], all optical signal processing [29], radio over fiber [30,31], cable access TV (CATV) [32] and low phase noise tunable photonic oscillators for time frequency applications [33,34]. Let us stress that P2 dynamics of the laser can also be used for accurate photonic microwave frequency conversion [35] for demultiplexing an individual channel in an optical time division multiplexing system. Other periodic dynamical states, such as period four and harmonic locking states can also be used for photonic microwave frequency conversion.

Because the extraction of all of the nonlinear dynamical features is highly meaningful for the above-cited applications, we also apply the clock recovery function to extract the waveform generated by P1 and P2 regimes of an optically injected semiconductor laser. The laser under study consists of an InAs/InP quantum dot (QD) Fabry-Perot laser emitting at 1560 nm and operating under weak optical injection. QD lasers have been predicted to have superior dynamical properties compared to QW or bulk lasers making them attractive candidates for applications such as high-speed sources in optical communication systems. In addition to low transparency current density and temperature-insensitivity of the threshold current, nanostructure lasers have also been touted to exhibit a larger linewidth enhancement factor (LEF), which in theory makes them very suitable for nonlinear dynamical studies based on injection-looking or optical feedback techniques [12,36].

The typical experimental setup is shown in Fig. 2. The ML is a continuous-wave external-cavity tunable laser, whose emission frequency and power can be controlled to vary the injection conditions (frequency detuning and power injection ratio). The light coming from

#205142 - $15.00 USD Received 21 Jan 2014; revised 4 Mar 2014; accepted 4 Mar 2014; published 27 Jun 2014

the ML is injected into the QD Fabry-Perot SL. The SL's threshold current I_{th} was measured under continuous waves to be about 110 mA at room temperature. During the entire injection-locking experiments, the pumping current is kept about $1.2 \times I_{th}$ while the injection ratio of the master laser to the slave laser is calculated to be $R_{ext} = 1.3$, meaning that the strength of the optical injection remains at a relatively low level. Optical injection is carried out in reflection mode, meaning that the light is injected into the facet from which the laser output is obtained. Therefore, a circulator is required to avoid instabilities in the ML The output signal of the SL is then detected with a 15 GHz photodiode, and sampled by a real-time oscilloscope at a 25 GSamples/s sampling rate. The bandwidth of the ADC is 20 GHz. The times series is then extracted using the technique described above and by varying the frequency detuning Δf, while the phase portrait is obtained by using the derivation of the average intensity field. The estimation of the frequency of the signal under test is done with 2^{14} samples. The optical and electrical spectra are monitored with a 10 pm optical spectrum analyser (OSA), and a 22 GHz bandwidth electrical spectrum analyser (ESA) coupled to a 10 GHz bandwidth photodiode.

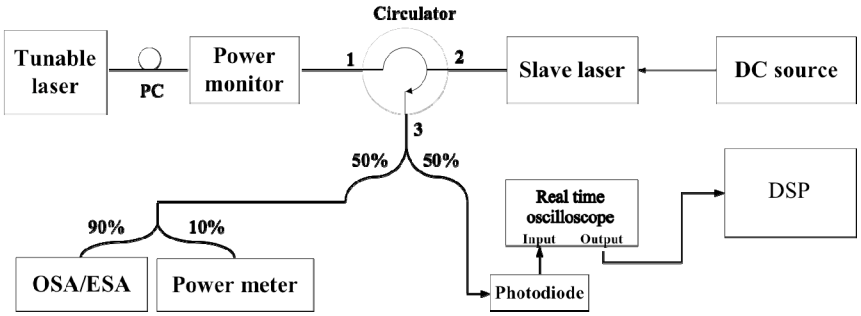

Fig. 2. Schematic showing the experimental setup used for the extraction of the dynamical regimes of an optically-injected QD laser. PC: polarization controller, OSA: optical spectrum analyser, ESA: electrical spectrum analyser, DSP: digital signal processing block.

Figure 3 depicts the experimental results obtained for the P1 dynamical state. Figure 3(a) shows the time series obtained after processing of the raw data. The field intensity of the injected QD laser is purely periodic as observed from the baseband spectrum (Power Spectral Density (PSD), Fig. 3(c)) with a measured oscillation frequency around 4.9 GHz. The phase portrait depicted in Fig. 3(b) confirms the single-frequency oscillation.

In Fig. 4, the results corresponding to the P2 dynamical regimes are depicted. Figure 4(c) exhibits a fundamental frequency around 2 GHz and the first harmonic close to 4 GHz. Its value is slightly lower than the frequency of the period one oscillation, which is a consequence of the different injection conditions. The P2 dynamical regime indicates that at least three spectral components oscillate in the laser cavity. Compared to the P1 dynamical regime, the repetition rate of the P2 regime is half, leading to a frequency spacing reduction. Hence, we expect an increase of the FWM efficiency. As opposed to the traditional FWM regime arising in the locking map [37], we guess that the P2 regime may also induce by FWM the generation of new spectral components in the side bands of the optical spectrum, and thus the presence of a second harmonic in the electrical spectrum as shown in Fig. 4c. Besides, the measured phase portrait has a very good accuracy and clearly exhibits a more complex trajectory.

#205142 - $15.00 USD Received 21 Jan 2014; revised 4 Mar 2014; accepted 4 Mar 2014; published 27 Jun 2014

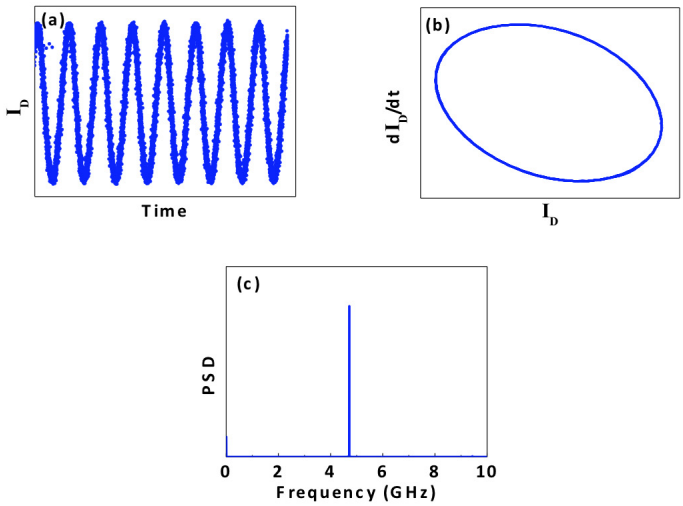

Fig. 3. Experimental measurement of P1 dynamical state: a) time series b) phase portrait and c) baseband spectrum (PSD: Power Spectral Density).

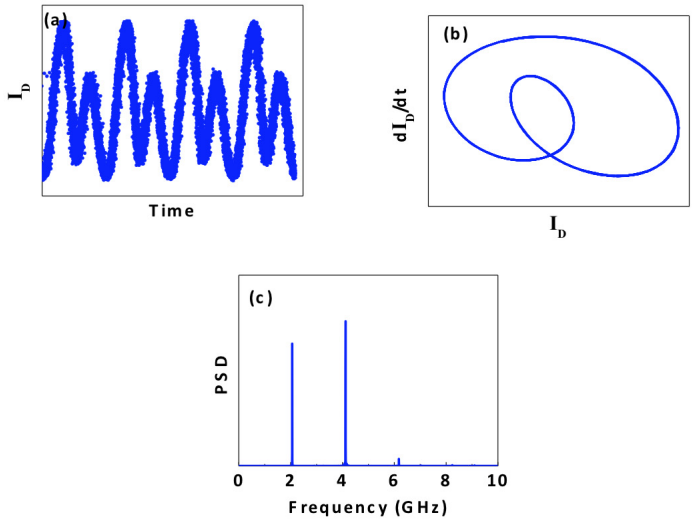

Fig. 4. Experimental measurement of P2 dynamical state: a) time series b) phase portrait and c) baseband spectrum (PSD: Power Spectral Density).

5. Measurement of dynamic properties in the presence of deterministic timing jitter

In the previous section, the sampling configuration corresponded to an over-sampling configuration, i.e. leading to the acquisition of more than one sample per period. The acquisition duration was short: 320 ns. In this context, the impact of timing jitter is reduced, allowing the short term monitoring of the signal under test. In this section, the sampling frequency is tuned to 6.25 GSamples/s, with total acquisition duration of about 70 µs, corresponding to the real-time acquisition of more than 400 kSamples. The duration of a set of 2^{14} samples required for the recovery of the periodicity is 2.6 µs, much longer than in the previous section. As a consequence, the impact of the timing jitter has to be taken into account in the analysis of the processed data used to display the periodic waveform.

#205142 - $15.00 USD Received 21 Jan 2014; revised 4 Mar 2014; accepted 4 Mar 2014; published 27 Jun 2014

Figure 5 shows the obtained periodic waveforms at several instants. We observe very different behaviour depending on the instant of observation. Thanks to the robustness of the proposed algorithm due to its block structure, the jitter assigned to each period-one time series is attributed to the signal generation method itself. The master laser is an external cavity laser (ECL) affected by a sine frequency drift. Its temporal characteristics had been measured with a time-resolved technique, with an amplitude of about 10 MHz and a frequency in the 10-20 kHz range. Numerical simulations confirmed the observed behaviour. The observed deterministic jitter is attributed to the frequency drift of the master laser.

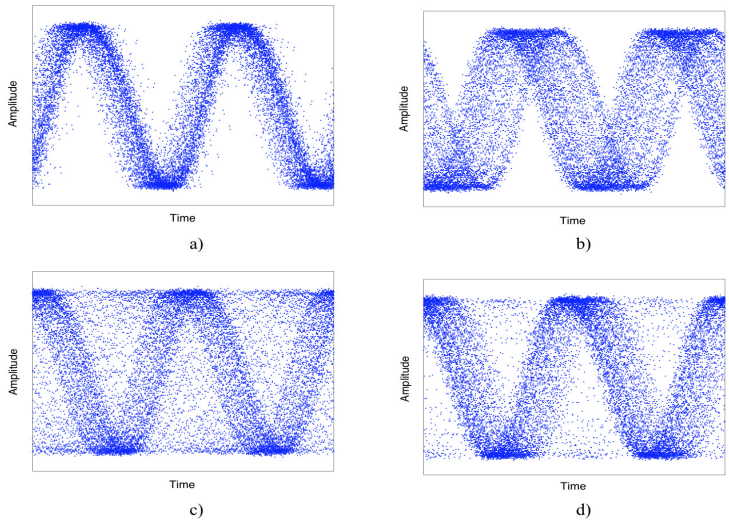

Fig. 5. Experimental measurements of P1 time series using low sampling frequency (6.25 GS/s, 2.6 µs block duration) for several instants within a 70 µs window: a) 5.2 µs b) 26 µs c) 47 µs and d) 60 µs.

6. Conclusion

In conclusion, in this paper we proposed a clock recovery algorithm to display periodic waveform as well as eye diagram from the measurement of asynchronous sampled signals. It allows recovering the periodicity of a modulated signal with an error estimation of the normalized temporal step of 10^{-5} with only 2^{14} samples. It provides very good performances for a time varying channel due to its block structure. This technique is applied to the characterization of the dynamical regimes of a signal generated by an optically-injected QD laser. The time series, as well as the related phase portraits, of the SL outputs are experimentally analysed. The proposed technique is meaningful since it does not require any time reference and interpolation operation. In addition, it also provides an accurate representation in the time domain and in the phase space of all the nonlinear dynamical features. Thanks to the large number of samples used to plot the time series, we have obtained a high resolution representation of the signal under test, representative of the analogue signal $I_D(t)$. This technique appears as a promising tool to investigate the nonlinear dynamics arising in semiconductor diode lasers with different gain media.

Acknowledgments

This work is supported by the "OCELOT" project, from the French national ANR program. The authors would also thank Dr. Ravi Raghunathan from Virginia Tech, USA for his careful reading of the manuscript. Dr. Frédéric Grillot's work is supported by the European Office of Aerospace Research and Development (EOARD) under grant number FA8655-12-1-2093. Cheng Wang's work is supported by China Scholarship Council.